Miniaturized bioactivity screening of complex samples

Heus, F.A.H.

2015

document version
Publisher's PDF, also known as Version of record

Chapter 3

An efficient analytical platform for on-line microfluidic profiling of neuroactive snake venoms towards nicotinic receptor affinity

Ferry Heus[1], Freek J. Vonk[2,4,5], Reka A. Otvos[1,3], Ben Bruyneel[1], August B. Smit[3], Henk Lingeman[1], Michael Richardson[2], Wilfried M. A. Niessen[1,6] and Jeroen Kool[1]

(1) Division of BioMolecular Analysis, Department of Chemistry and Pharmaceutical Sciences, Faculty of Sciences, VU University Amsterdam, De Boelelaan 1083, 1081 HV Amsterdam, The Netherlands
(2) Institute of Biology, Leiden University, Sylvius Laboratory, Sylviusweg 72, 2333 BE Leiden, The Netherlands
(3) Department of Molecular and Cellular Neurobiology, Center for Neurogenomics and Cognitive Research, Neuroscience Campus, VU University Amsterdam, De Boelelaan 1085, 1081 HV Amsterdam, The Netherlands
(4) School of Biological Sciences, University of Wales, Bangor L57 2UW, UK
(5) Naturalis Biodiversity Center, Darwinweg 2, 2333 CR Leiden, The Netherlands
(6) Hyphen MassSpec Consultancy, de Wetstraat 8, 2332 XT Leiden, The Netherlands

Toxicon, 2013. 61:112

Abstract

Venomous snakes have evolved their efficient venomous arsenals mainly to immobilize prey. The highly variable toxic peptides in these venoms target a myriad of neurotoxic and haemotoxic receptors and enzymes and comprise highly interesting candidates for drug discovery. Discovery of bioactive compounds from snake venoms, however, is a challenge to achieve. We have developed and applied a methodology to rapidly assess bioactives in a snake venom proteome. Our microfluidic platform opens up efficient and rapid profiling of venomous anti-cholinergic receptor compounds. The key advantages of our methodology are: (i) nano amounts of venom needed; and (ii) a direct correlation of selected bioaffinities with accurate mass. To achieve this, we have for the first time successfully constructed a functional post nano-LC split to MS and bioaffinity profiling. In our method, comprehensive venom profiles with accurate masses and corresponding bioaffinities are obtained in one analytical run and will subsequently allow immediate purification of bioactive peptides with LC–MS, guided by accurate masses of the bioactives only. We profiled several neurotoxic Elapidae snake venoms using our methodology in combination with the acetylcholine binding protein (AChBP) as biological target protein. The latter is a homologue of nicotinic acetylcholine receptors (nAChRs), a drug target in neurodegenerative diseases and cognitive decline such as Parkinson's and Alzheimer's, and in pain related diseases. Our methodology was evaluated and validated with high-affinity α-bungarotoxin and haemotoxic/proteolytic *Vipera ammodytes* venom spiked with α-bungarotoxin. Thereafter, the methodology was applied to profile the venom proteomes of *Dendroaspis jamesoni kaimosae*, *Naja annulifera* and *Naja nivea*. Gathering comprehensive profiling data took less than 2 h per snake venom measured. The data yielded 20 AChBP ligands of which the corresponding accurate masses were used to retrieve information from literature regarding their function and targeting specificity. We found that from these 20 ligands, 11 were previously reported on, while information on the others could not be found. From these 11 peptides, five have been reported to have nAChR affinity, while the others are reported as cytotoxic, cardiotoxic or as orphan toxin. Our methodology has the potential to aid the field of profiling complex animal venoms for drug discovery.

Introduction

Recent advances in the scientific understanding of diseases have raised hopes of an increase in the number of novel drugs reaching the market. Further, many potential disease-related orphan receptors are now being investigated. It is therefore disappointing to realise that the number of drugs reaching the market is actually dwindling. One of the solutions to this problem is the exploration of natural sources, such as animal venoms, using current analytical technologies to increase the numbers of potential new lead compounds. Why? Possible reasons: venoms are highly potent because they are under strong natural selection. Venoms contain multiple novel compounds, free from IP restrictions. They have also provided many new drugs or even new classes of drugs, in the past. In order to exploit this great natural resource, several challenges have to be resolved. These include bioanalytical challenges such

as: 1) the complex nature of the samples and the intrinsically time-consuming process of elucidation, 2) the occurrence of synergistic actions between components in a complex natural extract, and 3) sourcing adequate quantities, especially when screening animal venoms. For these and other reasons, pharmaceutical companies scaled down or even abandoned their natural extract drug discovery pipelines. Nevertheless, many drugs approved during the last decades are based on natural products [15].

Another potential reason for abandoning natural extract product pipelines is that most drug companies focused on plant and fungal derived bioactives [22], because these mostly small-molecule compounds fitted well in small-molecule drug discovery pipelines. Traditional problems with peptide and protein derived drugs are amongst others due to issues with (oral) drug administration, bodily distribution, e.g., limited crossing of the blood brain barrier, and immunogenicity issues, e.g., due to the difficulty of preparation. Advanced formulation methodologies and administration routes as well as current knowledge on immunogenicity and immunotoxicity have brought venom peptides back into consideration as candidate drugs. Some successful examples are Prialt (Ziconotide) derived from a predatory cone snail (*Conus textilus*) and used to treat severe chronic pain; Byetta (Exenatide) derived from the venom of the Gila monster (*Heloderma suspectum*) and used against diabetes type II; ACE inhibitors derived from the venom of the South American Lancehead snake (*Bothrops jararaca*) for the treatment of hypertension; and the antiplatelet drug Integrillin derived from the venom of the Saw scaled viper *Echis carinatus* [38] These examples justify the screening of venoms, including snake venoms, for compounds that might be a source for biopharmaceutical drug candidates. Furthermore, from a pharmacological point of view, venom peptides are also interesting. The acetylcholine receptor, for example, was discovered in 1970 by use of bungarotoxin as molecular probe.

One of the specific difficulties of effective natural-extract screening is the accurate and rapid bioactivity/identity correlation of bioactives with current traditional effect-directed analysis (EDA) methodologies [24]. EDA approaches are today's standard for bioactive mixture analysis and are widely applied in environmental [2, 17] and natural-product screening [8, 34, 40], as well as in animal-venom profiling [9]. In this approach, bioactive compounds are separated and subsequently fractionated, e.g., with liquid chromatography (LC), into a number of fractions, after which each fraction is tested for bioactivity. Ultimately, the bioactives are analysed with mass spectrometry (MS) to identify the active compounds. However, EDA studies often fail to identify the bioactive compounds, because even after repeated fractionation, biologically active fractions remain too complex for chemical identification, and in case of peptides also denaturation might occur. Additionally, the EDA workflow consumes large amounts of precious sample, especially in the case of venoms.

Even though some snake venom proteomes have been completely elucidated and sequenced, many toxins have unknown functions and protein targets. Of these “orphan toxins”, only a hypothesised functionality is known by sequence homologies with toxins having known bioactivities. Based on the large functional diversification followed by minor mutations in some of the toxin families, it is difficult to estimate function based on sequence similarity.

These toxins are often only classified broadly as cytotoxic, cardiotoxic or weak neurotoxic [11], with a myriad of different (unknown) receptors and proteins recognized or bound.

We recently developed a miniaturized screening methodology based on post-column on-line screening, sometimes called High Resolution Screening (HRS), for analysis of small compound libraries where nano-LC was hyphenated on-line to a microfluidic biochemical detector [16]. This methodology needed two analytical runs for analysis: the first run with nano-LC connected to the biochemical detector for assessing bioactivity of individual ligands, and the second run with nano-LC connected to MS for determination of the accurate masses of the eluting compounds. However, although this methodology would in theory allow for analysis of intrinsically low venom amounts, it is unsuited for profiling snake venoms as the complexity in this case overwhelms the analytical system. The main issue here is that the system is able to only assess bioaffinity in one run therefore necessitating a second nano-LC–MS analysis for peptide identification. Now, the main bottleneck becomes apparent as repeatability of nano-LC systems is by far not sufficient for the demanded precision in retention time of eluting peptides. Therefore, the bioactivity of peptides can never be correlated to their accurate masses effectively.

In the current work, we demonstrate a microfluidic screening methodology, with post-column bioactivity and parallel accurate mass analysis, for profiling neurotoxic snake venoms towards nicotinic receptor-like affinity. Towards this end, we have for the first time successfully constructed a functional post nano-LC split to MS and bioaffinity profiling. For correlation of eluting bioactives to their accurate masses, a nano-electrospray ionization MS (nano-ESI-MS) was placed in parallel with a microfluidic biochemical detector via a post-nanocolumn split. This miniaturized HRS approach was applied to efficient venom profiling of mainly Elapidae snake venoms. We used the acetylcholine binding protein (AChBP) as biological target protein. The AChBP is a homologue of nicotinic acetylcholine receptors, which are considered drug targets in neurodegenerative diseases and cognitive decline, such as Parkinson's and Alzheimer's, and in pain related diseases. The methodology was evaluated and validated with neurotoxin spiked *Vipera ammodytes* venom, a member of the Viperidae family known for having mainly hemotoxic/proteolytic peptides. Subsequently, the venoms of the Elapidae family species *Dendroaspis jamesoni kaimosae* (black tailed Jameson's mamba), *Naja (haje) annulifera* (African cobra) and *Naja nivea* (cape cobra) were comprehensively profiled. Most of the bioactives found could directly be correlated to their corresponding accurate mass.

Materials, methods and experimental

2.1. Chemical and biological reagents

Ls-AChBP (from snail species *Lymnaea stagnalis*) was expressed from *Baculovirus* using the pFastbac I vector in Sf9 insect cells and purified from the medium as described recently [4]. The fluorescent tracer ligand DAHBA, (E)-3-(3-(4-diethylamino-2-hydroxybenzylidene)-3,4,5,6-tetrahydropyridin-2-yl)pyridine, was synthesized in house [27]. NaCl, trizma base, HCl, 5% dimethyldichlorosilane (DMDCS), phospolipase A_2 (Uniprot #P00602) from *Naja mossambica* venom, muscarinic toxin-2 (P18328) from *Dendroaspis angusticeps* venom and α-bungarotoxin (α-BTX) from *Bungarus multicinctus* were purchased from Sigma–Aldrich, (Zwijndrecht, The Netherlands). Erabutoxin A (P60775) from *Laticauda semifasciata* and α-Cobratoxin (P01391) from *Naja kaouthia* were purchased from Latoxan (Valence, France). KH_2PO_4, Na_2HPO_4 and NH_4HCO_3 were obtained from Riedel-de-Haën (Seelze, Germany). I Nicotine (99.0%) was purchased from Janssen Chimica (Beerse, Belgium). Enzyme linked immunosorbent assay (ELISA) blocking reagent (ELISA-BR) was purchased from Hoffmann-La-Roche (Mannheim, Germany). [Met^5]-Enkephalin and human angiotensin I were purchased from Sigma–Aldrich, Mca-Lys-Pro-Leu-Gly-Leu-Dap(Dnp)-Ala-Arg-NH_2 from Bachem (Bubendorf, Switzerland). ULC/MS grade Trifluoroacetic acid (TFA; 99,95%) and acetonitrile (ACN; 99.97%) were purchased from Biosolve (Valkenswaard, The Netherlands). HPLC grade water was produced using a Milli-Q purification system from Millipore (Amsterdam, The Netherlands).

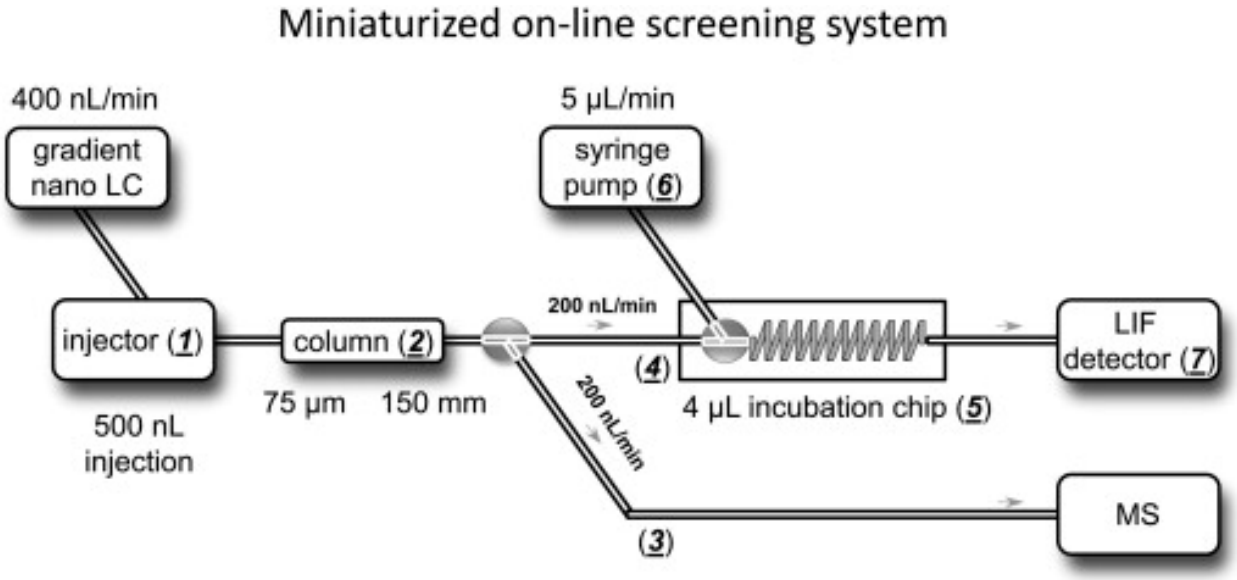

Figure 1. Schematic view of the complete microfluidic HRS setup. Venom is injected for analysis (***1***). After nano-LC (***2***), a split allows eluting toxin peptides to go to nano-ESI-MS for assessment of accurate mass (***3***) and to the biochemical assay (***4***) with help of a 1:1 post-nano-LC split. The on-line microfluidic biochemical assay was performed in a microfluidic chip (***5***) for which bioassay solution (***6***) containing AChBP and the tracer molecule DAHBA were infused continuously by a syringe pump at 5 µL/min and mixed in with nano-LC effluent running at 200 nL/min after the split, in the 4-µL open-tubular reaction chamber of the microfluidic chip. The chip's outlet was hyphenated to a bubble cell capillary (***7***) wherein light emanating from the high intensity LED was focused. Emitted light from the AChBP/DABHA complex was subsequently detected by the photomultiplier tube.

2.2. Instrumentation

2.2.1. Microfluidic confocal fluorescence detection system

The complete system consisted of a nano-LC unit with post-column split to an MS and an on-line chip functioning as biochemical reactor, where the LC flow and a bioassay solution were mixed, and a microfluidic LED based LIF detector as described by Heus et al. [16]. The complete system is schematically shown in Figure 1.

2.2.2. Nano-LC and solvent delivery system

The Ultimate nano-LC system with a Famos autosampler was from LC Packings (Amsterdam, The Netherlands). The system was operated at 400 nL/min. Mobile phase solvent A consisted of water and 0.1% TFA and solvent B of ACN and 0.1% TFA. Sample volumes of 500 nL were injected into the analytical capillary column (150 mm × 75 μm internal diameter (i.d.)) packed in-house with Aqua C18 particles (particle size 3 μm, 200 Å pore diameter; Phenomenex, Torrance, CA, USA). For venom analysis, a 90-min gradient elution was applied running 5 min isocratic at 5% solvent B, then rising to 15% solvent B in 10 min, followed by a rise towards 45% solvent B in 60 min, whereafter solvent B was set to reach 70% during 10 min, running isocratically at 70% for 5 min. To prevent particulate matter to clog the capillary column, the column inlet was connected to a low dead volume union containing a filter capsule (type M 572 and M 128 respectively, Upchurch Scientific, Oak Harbor, WA, USA). The column exit was connected to a low void volume T-connector where the effluent was split to the MS and the on-line bioassay by two pieces of bare fused silica (1000 mm × 10 μm i.d.). All fused-silica capillaries used for connections to and from the chip were purchased from BGB Analytik AG (Schloßböckelheim, Germany).

2.2.3. Microfluidic chip

The microfluidic chip and the chip holder (type 4515), produced by Micronit Microfluidics, (Enschede, The Netherlands), was described in detail elsewhere [16]. The open-tubular microreactor had a total volume of 4 μL. The reactor had two inlets and one outlet. One inlet was used to connect the nano-LC carrier flow; the other inlet to infuse the AChBP and tracer ligand DAHBA [16, 27] at a flow rate of 5 μL/min by a Model 980532 syringe pump (Harvard Apparatus, Holliston, MA, USA). The chip outlet was connected via a deactivated fused-silica capillary to the microfluidic LIF detector, as described [16].

2.2.4. Microfluidic LED based LIF detector

The flow cell of the detector consisted of a 150 μm i.d. extended light path “bubble cell” with 50 μm i.d. connecting capillaries (G1600 64232, Agilent Technologies, Amstelveen, The Netherlands). This bubble cell served as the actual flow-through detector cell. Light emanating from a high-intensity LED passed a 465 nm single band pass filter, was collimated by a lens, reflected by a dichroic mirror under 90° and focused into the centre of the bubble cell by a 20 × quartz microscope objective. Emitted light passed the same dichroic mirror, a focussing lens, and a 520 nm single band pass filter, after which it was detected by photomultiplier tube. A detailed description of this detector can be found elsewhere [16].

2.2.5. Nano LC MS

A Shimadzu ('s Hertogenbosch, The Netherlands) ion-trap–time-of-flight (IT–TOF) hybrid mass spectrometer equipped with a Picoview nano-ESI source from New Objective (Woburn, MA, USA) was operated in positive-ion mode. A 40 mm × 180 μm o.d. × 30 μm i.d. stainless-steel emitter was used (ES522, Proxeon/Thermo Scientific, Waltham, MA, USA), functioning as the spray needle. The spray needle was connected to the nano-LC system via a 1000 mm × 10 μm i.d. bare fused-silica capillary by a low void volume connector (type P 720, Upchurch Scientific) which was integrated in the nano-ESI source. The temperature of the heating block and curved desolvation line were set to 200 °C. The interface voltage was set at 1.7 kV, resulting in a current of ~32 μA.

2.3. Biochemical assay and samples

2.3.1. Biochemical assay

Fresh solutions of 5 nM Ls-AChBP and 15 nM DAHBA were made every day by dissolving in a bioassay solution containing 1 mM KH_2PO_4, 3 mM Na_2HPO_4, 0.16 mM NaCl, 20 mM trizma base/HCl at pH 7.5 and 400 μg/mL ELISA BR. The bioassay solution was housed in a 2.5 mL syringe (type 1002LTN, Hamilton, Bonaduz, Switzerland) which was kept at 4 °C. The on-line bioassay itself was performed at 22 °C [16].

2.3.2. Snake venoms

Lyophilized venoms samples of *Naja annulifera, D. jamesoni kaimosae* and *N. nivea* were acquired as described very recently [38]. *V. ammodytes* venom was purchased from Sigma–Aldrich. 2–3 mg of lyophilized crude venom sample was dissolved in water/ACN/TFA 95:5:0.1% at a concentration of 10 mg/mL and subsequently centrifuged at 13,400 rpm for 10 min to remove particulate matter. Aliquots of these samples were stored at −20 °C until further use. Before analysis, 40 μM internal standard nicotine was added together with three peptides at 2 μM each. The resulting venom solutions were directly injected in duplicate onto the nano-LC system for parallel bioaffinity screening and MS identification. Samples were re-analysed at lower or higher concentrations whenever necessary. Nicotine served as an internal standard and for alignment between the MS chromatograms and the bioassay readout. In the same way, the three reference peptides served to align MS data between different runs, whenever necessary. The three peptides were [Met^5] enkephalin, human angiotensin I and Mca-Lys-Pro-Leu-Gly-Leu-Dap(Dnp)-Ala-Arg-NH_2, which were detected at *m*/*z* 627.146, 648.848 and 611.307 respectively. In the figures, these peptides are numbered 1, 2 and 3.

3. Results and discussion

This work describes the use of an efficient analytical platform for the profiling of neurotoxic snake venoms. The technology is based on an HRS approach in which the on-line biochemical assay assesses bioactivity towards Ls-AChBP, mimicking predominantly neuronal nAChR binding. Parallel MS analysis provides accurate masses of the bioactive peptides. We choose for a miniaturized nano-LC setup to meet the challenge of a limited amount of venom often available per snake species, and to provide sufficient sensitivity. This miniaturized setup was developed previously by using an on-line microfluidic chip (4 μL) and nano-LC [16]. In the current setup (Fig. 1), an additional post-column split is introduced directing half of the 400 nL/min effluent from the nano-LC to the nano-ESI interface. The other half is directed to the microfluidic chip where it is mixed continuously with the bioassay solution, which is infused at 5 μL/min by a syringe pump. The outlet of the chip is connected to the confocal LED induced fluorescence detector, which monitors bioaffinity of the eluting toxins after in flow incubation. The bioassay is based on fluorescence enhancement in which the tracer ligand DAHBA shows increased fluorescence yield upon binding to the AChBP. As an eluting peptide competes with DABHA for Ls-AChBP binding, a negative peak in the signal is observed. Identified bioactives could, if desired, subsequently be purified in a straightforward fashion by normal-bore LC–MS, only guided by the accurate mass of the peptides for further pharmacological studies on nAChRs.

3.1. Method evaluation for the screening of snake venoms

In order to evaluate the applicability and performance of the miniaturized methodology for the screening of bioactive peptides in snake venom, a standard addition study was performed first, to assess sensitivity, reproducibility, correlation of peak shapes observed in MS and the biochemical assay, and (post-column) band broadening. This was done by injecting 5 μg of *V. ammodytes* (sand viper) venom solution in a 500 nL sample containing increasing amounts of α-bungarotoxin (α-BTX). *V. ammodytes* venom is primarily hemotoxic, thus not containing abundant neurotoxic peptides with probable affinity towards Ls-AChBP. In this way, the highly active spiked α-BTX was studied in a complex venom matrix, although without other significant bioactives. This allowed determination of whether the HRS system is capable of pinpointing a single neurotoxic peptide amongst hundreds of other (mainly non-neurotoxic) peptides. Furthermore, this part of the study gives information on the expected limits of detection (LODs) for the venom toxins with respect to their biochemical and MS detection.

As can be seen in Figure 2A and B, α-BTX elutes from the reversed-phase LC column as two isoforms in 4 peaks, a separation profile previously reported by others [5, 10]. This profile can be easily mistaken for being 4 different peptide species as four peaks are observed, but due to correlating peak shapes between the biochemical and the MS detection, misinterpretations like this are avoided. The results depicted in Figure 2 clearly emphasize one of the main advantages of this methodology. In contrast to reversed-phase LC separations of reduced and unfolded peptides in proteomics studies, the LC elution profiles of intact small proteins often do not give single sharp peaks. Nevertheless, the bioaffinity can be correlated to

corresponding accurate masses. With the highest amount of spiked α-BTX (250 ng, absolute amount injected), the biochemical assay became saturated, indicating that practically all DAHBA tracer ligand was displaced from Ls-AChBP (Fig. 2A, trace E). It was found that the LOD of the high-affinity ligand α-BTX (K_d of 8.59) [36] was ~2 ng (Fig. 2A, Trace B) in the biochemical assay and ~25 times higher with MS.

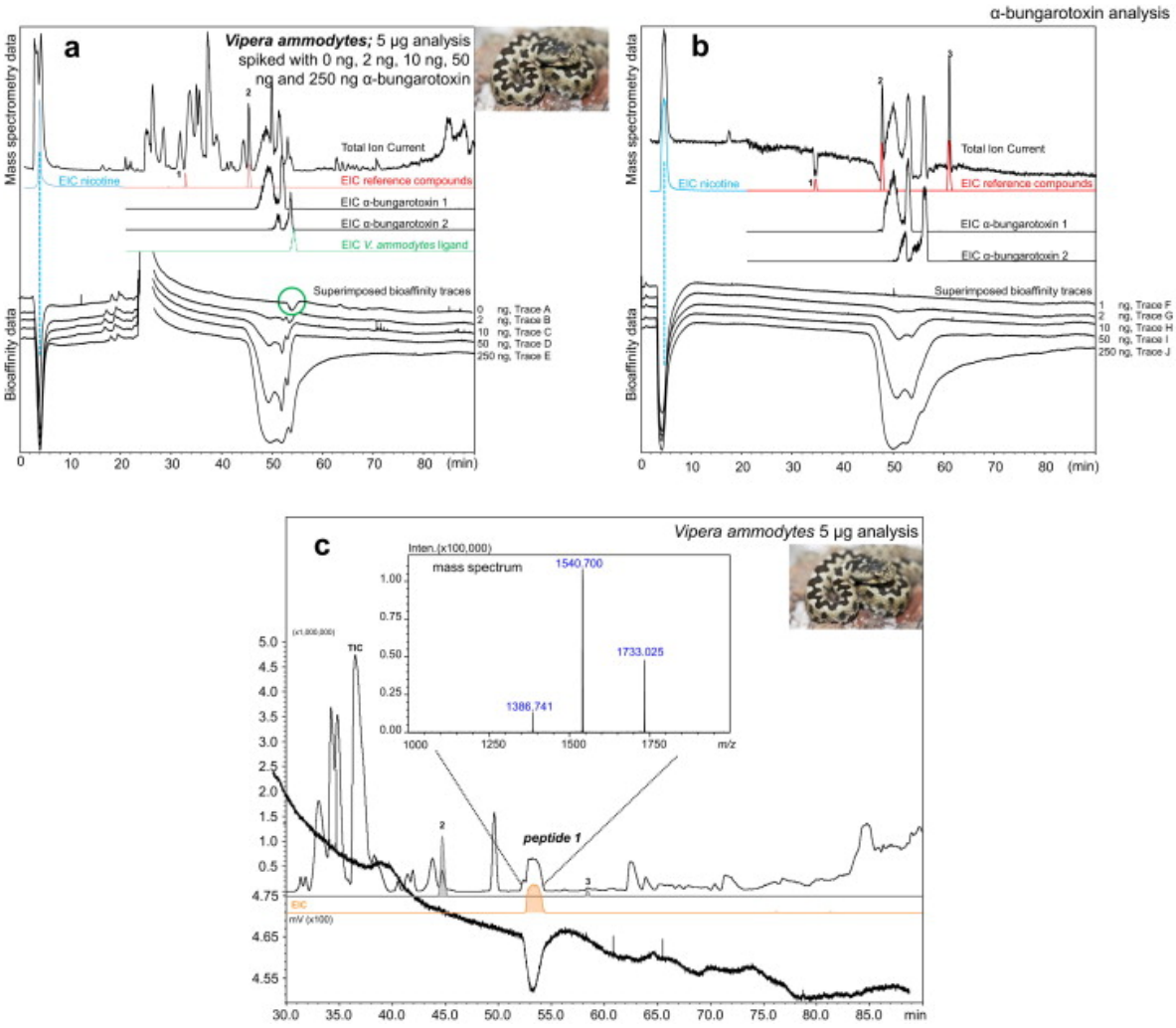

Figure 2. The applicability and performance of the analytical setup was evaluated by injecting 5 µg of *Vipera ammodytes* venom, spiked with increasing amounts of α-Bungarotoxin (α-BTX) (Fig. 2A). The mass spectrometric data represents the data obtained for the *V. ammodytes* venom spiked with 250 ng α-BTX. Shown are the total ion chromatogram (TIC) of the spiked *V. ammodytes* venom and the extracted ion chromatograms (EICs) of α-BTX (isoforms 1 and 2 which both elute as two peaks, as also previously reported in literature). Reference peptides allow for alignment with other chromatographic systems. The superimposed bioaffinity data represent 5 injections of the *V. ammodytes* venom with 0 ng, 2 ng, 10 ng, 50 ng and 250 ng α-BTX (trace A, B, C, D and E respectively). The venom analysis without α-BTX (trace A) obtained a previously unreported *V. ammodytes* ligand as is marked by the circle (corresponding EIC is also shown). Nicotine was added for alignment of the mass spectral data with the bioaffinity data. As part of the applicability and performance evaluation of the analytical setup also increasing amounts of α-BTX were injected without 5 µg of *V. ammodytes* venom. The resulting chromatograms from 1 ng, 2 ng, 10 ng, 50 ng and 250 ng α-BTX (trace F, G, H, I, and J respectively) injected are shown in Figure 2B. Chromatographic and mass spectrometric performance where comparable to Figure 2A,, while the bioaffinity data clearly showed the absence of the *V. ammodytes* ligand. Figure 2C shows the *V. ammodytes* ligand found (*peptide 1*) obtained from the 5 µg *V. ammodytes* venom analysis. The most abundant charge state corresponds to total peptide mass of 13,857 Da. Reported Viperidae neurotoxic phospholipases in this mass range typically contain 7 disulfide bridges. Hence, the nominal mass of this ligand is 13,871 Da. Inserted is the mass spectrum of the *peptide 1*, showing the 10×, 9× and 8× charged states (*m/z* 1386.741, 1540.700 and 1733.025 respectively).

Although the system showed to be very reproducible, sometimes retention times shifted slightly, especially when samples were repeatedly measured over several days. This is a known issue with nano-LC systems, but in our case did not impose serious problems as the biochemical data and MS data were measured simultaneously and despite the shifting retention times, the correlation remained accurate. Additionally, three reference peptides were introduced to enable alignment of chromatograms from different runs, and to allow for convenient transfer of the methodology and samples analysed to other laboratories, if necessary. α-BTX was also analysed separately without the viper venom. This resulted in similar biochemical detection signals, while only α-BTX peaks were observed in the LC MS data (Fig. 2B). These data confirm that the biochemical assay gives similar results for α-BTX, whether present in a complex venom sample or injected separately, thus also ruling out matrix effects. Finally, in these standard addition experiments, a viper venom peptide was found with affinity for Ls-AChBP, as is observed in the in Figure 2 trace A, and discussed below in Section Snake venom analysis, snake 1; *Vipera ammodytes*. The latter peptide was also observed when a blank sample only containing viper venom was analysed (Fig. 2C).

To evaluate the specificity of the screening system regarding AChBP binding, several isolated toxins associated with different physiological targets (besides neuronal nAChRs) were analysed by injecting them at increasing concentrations in the system. As described above, this was done with α-BTX, a model α7 nAChR binder. Other known high affinity ligands are the α-cobratoxins. As can be seen in Figure S1A (see Supplementary material), a 2 μg injection of α-cobratoxin (P01391) from *N. kaouthia* obtained a large bioaffinity signal as expected. The bioaffinity was so large that the system was overloaded for more than a day. After thorough flushing of the system, a 50 ng amount of α-cobratoxin was injected. Now the system was overloaded for a few hours after which the signal came slowly back to basal level. To validate the PLA_2 binding signal obtained in the viper venom analysis with a PLA_2 from another species, 5 μg of PLA_2 (P00602) from *N. mossambica* venom was analysed.

This phospholipase also showed low affinity AChBP binding (Supplementary Figure S1B). Additionally, several types of ‘short chain’ toxins were analysed that are classified as cardiotoxin or as ligands of the muscarinic receptors (mAChRs) and postsynaptic (muscle type) nAChRs. The Muscarinic toxin-2 (P18328) from *D. angusticeps* showed no bioaffinity signal at a concentration of 1 μg. The analysis of 5 μg muscle type α1 nAChR binder Erabutoxin A (P60775) from *L. semifasciata* did not show binding. We also screened a purified IMI conotoxin (P50983) from *Conus imperialis* and found it to indeed be a high affinity binder on AChBP (see Supplementary Figure S1C). These experiments investigating the specificity of the on-line AChBP screening platform indicated specificity to α-BTXs, α-cobratoxins and (certain) CTXs.

3.2. Snake venom analysis

3.2.1. Background

Snake venom proteomes comprise a complex cocktail of peptides, which during millions of years of evolution, evolved into highly active ligands towards enzymes and receptors. In general, the Viperidae family geared its venom to affect the function of various blood components, while the family Elapidae (including several species from the *Colubrid*

colubrinae subfamily) mainly developed a venom system with neurotoxic and cardiotoxic peptides (although this is no golden rule and there are exceptions). The three-finger toxins (3FTX) – a major and diverse family of low molecular weight (<10 kDa) neurotoxins – share as common tertiary that structure the main body which is shaped by four disulfide bridges, truncating the amino acid sequence in such a way that three loops are formed. All extant members have retained their peculiar "three-finger" molecular scaffold whilst exhibiting a diversity of different functions. However, despite retaining the common three-finger motif, members of this family have since evolved a myriad of different functions including effects on platelet function, different receptors associated with neurotransmission, ion channels, viability of cardimyocytes and red blood cells, mitosis and apoptosis; and effects on the cell membrane. The different 3FTX members also vary considerably in binding affinity for the different receptors and are important research ligands for studying receptors. Homologous 3FTXs are found in all advanced snakes: Elapidae (cobras and relatives), Viperidae (vipers and pitvipers), and others.

As the structural feature of 3FTXs resembles three fingers, these toxins belong to the 3FTX peptide family [23]. Not only their tertiary structure, but also their chain length is similar. Type I (or short chain) neurotoxins and cardiotoxins usually contain 60–62 amino-acid residues, while the Type II (or long chain) neurotoxins comprise 70–80 amino acids [23]. Furthermore, these peptides show 40–50% amino-acid sequence homology. The target affinities of these peptide toxins are 'tuned' by mutations in the extremities of the three loops, as this is where interactions with protein targets take place. For the neurotoxic peptides, the amino acids in the 'fingertips' of Loops I and II are most determining. Type I and Type II neurotoxins bind competitively to (postsynaptic) nicotinic acetylcholine receptors (nAChRs). These neurotoxins are commonly known as α-neurotoxins (α-NTXs) [9, 33]. Besides an elongated c-terminus, the Type II α-NTXs differ from Type I by an additional disulfide bridge at the extremity of Loop II. This difference causes the Type I α-NTXs to mainly target muscle α1 nAChRs, while Type II α-NTXs also target α7 nAChRs. The cardiotoxic (CTX) peptides are essentially cytotoxic peptides as they disturb membrane structures of a range of excitable and non-excitable cells [15]. Most likely, similar to the neurotoxins, there is a wide range of receptors and (ion) channels targeted by the CTX peptides [6, 25, 29].

Although mainly α-neurotoxins from Elapidae have been associated with nAChR binding, toxins from the Viperidae have also been reported to show (low) nAChR affinity. In these venoms, phospholipases A_2 (PLA_2s) rather than 3FTXs are responsible for the neurotoxic effects. This family of toxins typically contains seven disulfide bridges and a peptide chain length of 115–139 amino acids. Gorbacheva et al. [12] reported that crude viperid venoms also block nAChRs (and voltage gated Ca^{2+} channels) in isolated identified neurons of *L. stagnalis*. Subsequently, they showed that an isolated PLA_2 called Bitanarin has affinity for human α7 and *Torpedo californica* nAChRs, as well as for the AChBP (from *L. stagnalis*). This novel ligand is structurally similar to (smaller) PLA_2s and shows PLA_2 like activity, although it has 14 disulfide bridges and a peptide chain length of 138 amino acids [39].

3.2.2. Explanation of the table containing the comprehensive screening results

All snake venom peptides found to be bioactive towards the AChBP during this study are listed in Table 1. Mass correlations with literature via the Universal Protein Resource Knowledgebase (Uniprot) were made when found; literature references are referred by their accession number for convenient referencing. Most toxins have cysteine bridges and we measured the intact peptides. Since Uniprot and most literature give nominal masses from the reduced peptides, the known difference in molecular mass (2 Da per cysteine bridge) was taken into account when the number of cysteine bridges was known. In our case, most of the known bioactive peptides found had 4 or 5 cysteine bridges, implying a molecular mass difference of 8 or 10 Da, respectively. The toxin nomenclature used for the identified toxins, by correlation of nominal masses of bioactive peptides found per snake with literature, was done according to Fry et al. [11], and/or given as Uniprot identifier for easy reference. When a peptide could not be mass correlated with Uniprot, estimation on the protein family, amount of cysteine bridges and nominal mass were based on the peptide's mass (range).

3.2.3. Snake 1; Vipera ammodytes

As discussed in the method evaluation section, a viper ligand was detected from a 5-µg total venom sample of *V. ammodytes*. Figure 2C shows both the MS data (including the EIC and the mass spectrum of this AChBP ligand) and the biochemical detection signal of this analysis. Upon increasing concentrations of α-BTX, this viper bioactive is quickly masked by the highly active α-BTX standard. Table 1 shows mass spectrometric information of this ligand, which could not been traced back via Uniprot, and is called *peptide 1*. For full sequence identification, subsequent proteomics analysis guided by the accurate mass found should be conducted, and/or purification guided by the accurate mass. These analyses, however, are beyond the scope of the current work.

Table 1.
Snake toxins exhibiting Ls AChBP binding. The tables shows the accurate mass of the most abundant charge state of each bioactive peptide, the corresponding nominal peptide mass, the toxin family the peptide belongs to (when identified and known), the corresponding Uniprot accession number and their possible mechanism of action. All peptide masses reported in the table and in the following discussion are nominal masses and are correlated with masses found in Uniprot by searching the venom proteomes of the respective snakes profiled. Peptides not correlated in this way are referred to as '*peptide #*'.

Species	Most abundant isotope pattern		~Nominal mass	Protein family; sub-family	Peptide # or Uniprot #	# Disulfide bonds; ~ reduced mass	Molecular function
	m/z	Charge state					
Vipera ammodytes	1540.701	9	13,857.309	*Unknown* (PLA_2)	*Peptide 1*	*Unknown* (7; 13,871)	Unknown
Dendroaspis jamesoni	1121.021	6	6720.126	3FTX; Type IA NTX	P01417	4; 6729	α1 AChR inhibitor
Dendroaspis jamesoni	1159.085	6	6948.510	*Unknown* (3FTX)	*Peptide 2*	*Unknown* (4; 6957)	Unknown
Dendroaspis jamesoni	1124.405	6	6740.430	*Unknown* (3FTX)	*Peptide 3*	*Unknown* (4; 6748)	Unknown
Dendroaspis jamesoni	1232.229	6	7387.374	3FTX; Orphan group XIX	P25682	5; 7398	Unknown/toxin
Dendroaspis jamesoni	1766.309	8	14,122.472	*Unknown* (PLA_2)	*Peptide 4*	*Unknown* (8; 14,138)	Unknown
Dendroaspis jamesoni	1416.428	6	8492.568	*Unknown* (3FTX)	*Peptide 5*	*Unknown* (5; 8503)	Unknown
Dendroaspis jamesoni	1357.036	5	6780.180	*Unknown* (3FTX)	*Peptide 6*	*Unknown* (4; 6788)	Unknown
Dendroaspis jamesoni	1353.840	5	6764.200	3FTX; Orphan group XI	P01406	4; 6772	Unknown/toxin
Dendroaspis jamesoni	1395.485	5	6972.425	*Unknown* (3FTX)	*Peptide 7*	*Unknown* (4; 6980)	Unknown
Dendroaspis jamesoni	1328.074	5	6635.370	3FTX; Type IA NTX	P01418	4; 6743	α1 AChR inhibitor
Naja annulifera	1563.300	5	7811.500	3FTX; Type IIA NTX	P25674	5; 7821	α7 AChR inhibitor
Naja annulifera	1367.719	5	6833.595	3FTX; Orphan group XV	P62390	4; 6842	Cardiotoxin
Naja annulifera	1359.890	5	6794.450	3FTX; Type IA CTX	P01461	4; 6802	Cardiotoxin
Naja nivea	1316.441	6	7892.646	3FTX; Type IIA NTX	P01390	5; 7902	α7 AChR antagonist
Naja nivea	1338.750	5	6688.750	3FTX; Type IA CTX	P01456	4; 6697	Cardiotoxin
Naja nivea	1370.864	5	6849.320	*Unknown* (3FTX)	*Peptide 8*	*Unknown* (4; 6857)	Unknown
Naja nivea	1373.651	5	6863.255	3FTX; Type IA CTX	P01463	4; 6871	Cardiotoxin
Naja nivea	1380.115	5	6895.575	*Unknown* (3FTX)	*Peptide 9*	*Unknown* (4; 6904)	Unknown
Naja nivea	1367.715	5	6833.575	3FTX; Type IA NTX	P68419	4; 6842	α1 AChR inhibitor

3.2.4. Snake 2: Dendroaspis jamesoni kaimosae

From a 5-µg venom injection of the *D. jamesoni kaimosae* (Jameson's mamba), eight AChBP ligands were detected in the biochemical detection signal (Fig. 3A). The first (weak) binder, eluting at 33 min, can be mass correlated to a peptide (P01417) first reported by Strydom in 1973 [37] as a (weak) nAChR neurotoxin based on anti-venom affinity for the homologous cobra venom. Fry et al. classified it as a Type I α-NTX. The bioactive peak at 39 min is caused by two peptides (*peptide 2* and *peptide 3*) which could not be mass correlated with literature. The fourth affinity peak at 44 min was attributed to either co-eluting P25682 or *peptide 4*. P25682 has been classified by Fry et al. as an orphan toxin XIX (a group of *Dendroaspis* and *Bungarus* toxins of unknown function/protein target). The onset of binding signal at 48 min is probably caused by *peptide 5*, whereas the remaining signal is caused by P01406, which has been classified as an orphan group XI toxin (of unknown function/target) (Fry et al.) In between *peptide 5* and P01406, another a low abundant unknown peptide (*peptide 6*) elutes, which might responsible for (part of) the binding signal. P01406 elutes in two forms, also causing another binding signal at 55 min. The small binding signal at 62 min is caused by *peptide 7*, whereas the last signal at 77 min can be attributed to P01418, which has been classified as a Type I α-NTX (Fry et al.). A lower 1.7-µg venom injection provided better chromatographic peak shapes enabling more straightforward correlations (Fig. 3B). In conclusion, the majority of the peptides found in the *D. jamesoni kaimosae* require subsequent purification of the unknown co-eluting peptides followed by comprehensive functionality assaying and sequencing. This, however, is beyond the scope of the current work.

3.2.5. Snake 3: Naja annulifera

From a 5 µg *N. annulifera* (African cobra) venom injection, clearly three binding signals can be observed (Fig. 4A). The two binding signals eluting at ~ 65 min can be attributed to P62390 and P01461, first reported by Joubert et al. in 1976 [21]. The latter has been classified a Type IA cytotoxin (Fry et al.). The binding peak shows that possibly more Type IA cytotoxins exhibit α-neurotoxicity. P62390 has not been classified by Fry, but by sequence similarity it mostly resembles the ‘orphan group XV’ toxins (via Blast search in Uniprot), a group coined with only limited known biochemical function besides probable ‘low level cytotoxicity’ for *Naja* toxins (Fry et al.). P62390 shares, for instance, 90% homology with P1541, a *N. kaouthia* toxin classified as orphan group XV type (Fry et al.). As the MS signals of these peptides are quite high, while the affinity signals are (relatively) low, P62390 and P01461 are probably low affinity binders. Based on the same criteria, the main ligand eluting between 40 and 50 min is a low-abundant, high-affinity ligand. From the initial analysis at pH 2.5, two co-eluting ligand peptides were identified, which could be mass correlated with P25674 and P01399 from *Naja haje haje* (Egyptian cobra). When repeated at pH 7.5, P25674 and P01399 showed improved resolution (Fig. 4B). In addition, the MS intensity of peptide P25674 increased, making correlation with the bioaffinity signal more straightforward. P01399 was first reported by Joubert et al. in1975 [20] and classified as a weak cytotoxin. A homologue of this peptide has also been found in the *Naja sputatrix* (Indonesian spitting cobra (Q802B2); with 82% homology) and is reported as a weak (muscle type) nAChR ligand [18].

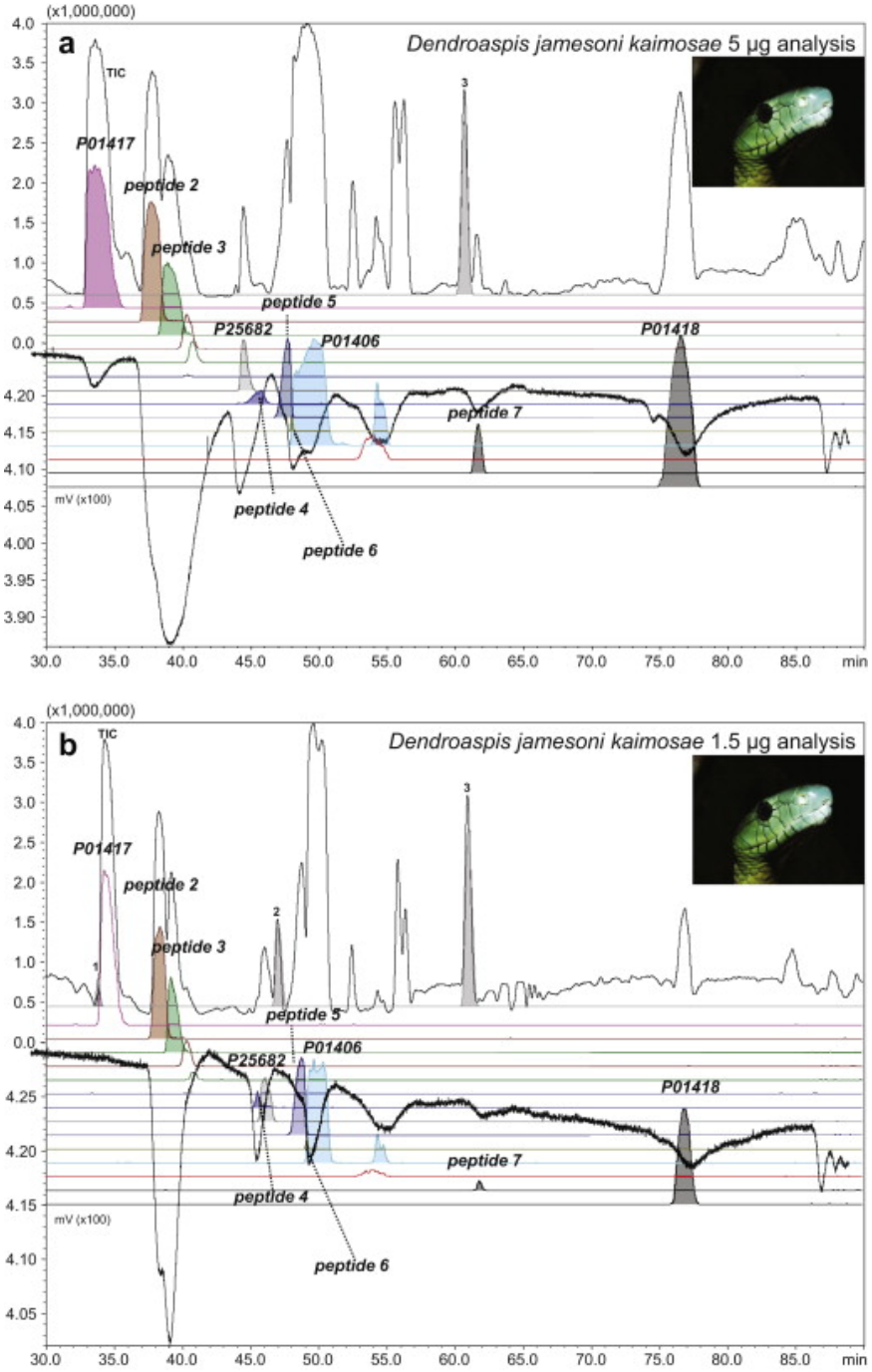

Figure 3. Typical result of a crude snake venom analysis where 5 µg (A) of *Dendroaspis jamesoni kaimosae* (Jameson's mamba) was injected. This analytical run obtained 10 ligands of which 4 were previously reported on in literature; classified as either muscle-type neurotoxin (P01417) or orphan ligand (P25682, P01406 and P01418). The venom analysis was repeated with a 1.67 µg injection (B) to provide for better chromatographic peak shapes enabling more straightforward correlations. Consequently, less ligands were detected at this venom concentration as some lower affinity neurotoxins reached their level of (biochemical) detection.

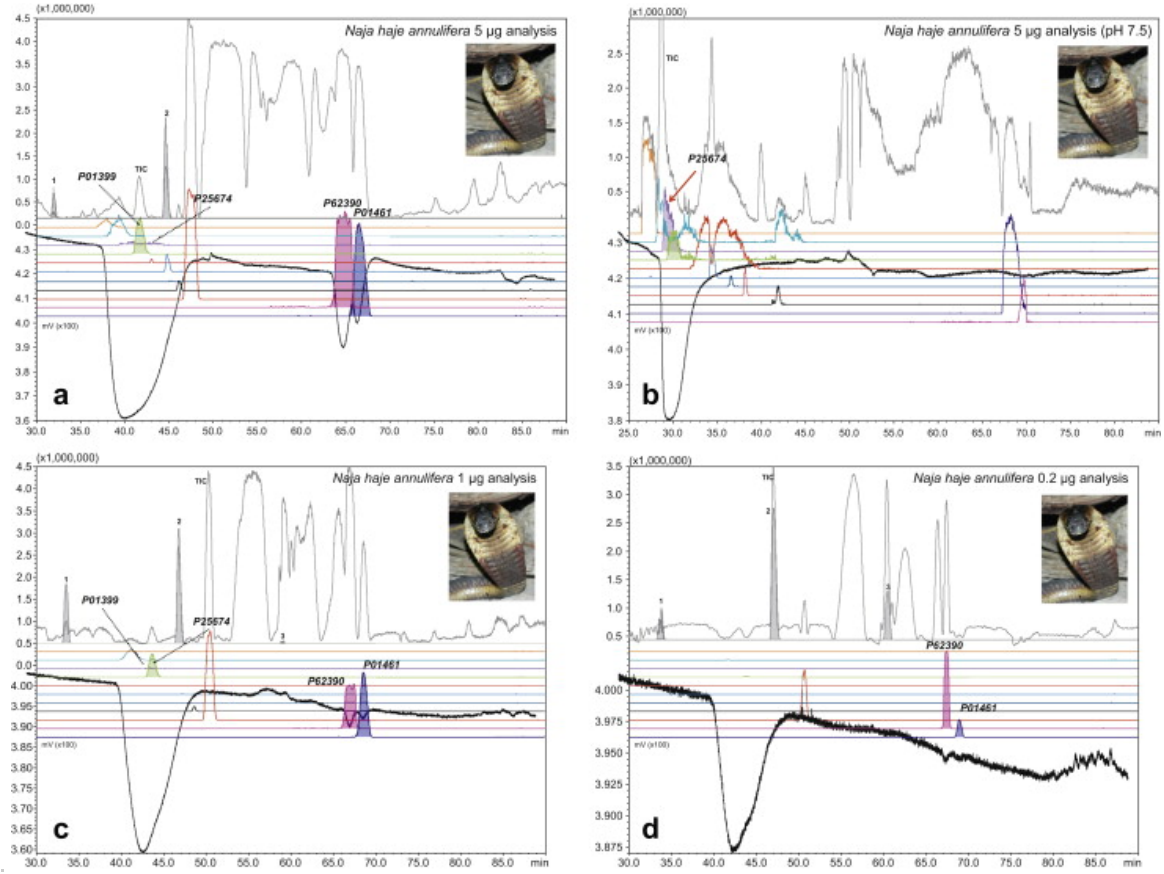

Figure 4. An analysis of 5 µg *Naja annulifera* venom obtained three binding signals (A). The first, large binding signal can be attributed to a highly active α-cobratoxin ligand P23474 (a toxin which has been reported in the highly homologues venom of *Naja haje haje*). The two latter binding signals were correlated to P62390 and P01461 (previously classified as Type IA cytotoxins). As the α7 nAChR ligand P25674 co-elutes with toxin P01399, the analysis was repeated at pH 7.5 (B). P25674 and P01399 showed improved resolution and the MS intensity of peptide P25674 increased. Again, this clearly shows the value of the higher pH analysis 'mode'. The analysis was thereafter repeated by injecting 1 µg and 0.2 µg venom (C and D respectively), which not only allows for more precise correlation between the MS and bioaffinity data sets, but also demonstrates the repeatability of the system.

The main neurotoxic ligand in the *N. annulifera* venom, P25674, was identified by its homologue reported in the *N. haje haje* venom, which contains a peptide with an identical mass and has been reported as a highly active α7 ligand [19].As these cobra subspecies share many homologues toxin peptides, it can be assumed that this particularly high-affinity peptide has been 100% conserved in sequence in both species. On the other hand, as it known that in the 1970s and 1980s many venoms came from species that were misidentified [35], it cannot be ruled out that the *N. haje haje* venom used [19] was in fact *N. annulifera* venom. Figure 4C and D show the results of the venom injected in lower amounts (1 µg and 0.2 µg) to provide better chromatographic signals allowing for more reliable biochemical correlations. This was indeed observed. The caveat mentioned earlier and also the rationale for injecting a high amount of venom for analysis: the major bioactive was not observed in MS anymore when looking at the amount of 0.2 µg injected (Fig. 4D). This can easily lead to misinterpretations. Therefore, in some cases, like the one described here, different concentrations are to be analysed in order to reach a high confidence regarding correlation of bioactives to their identity. As one additional analytical run with a lower concentration injected takes less than 2 h, this is not a significant problem.

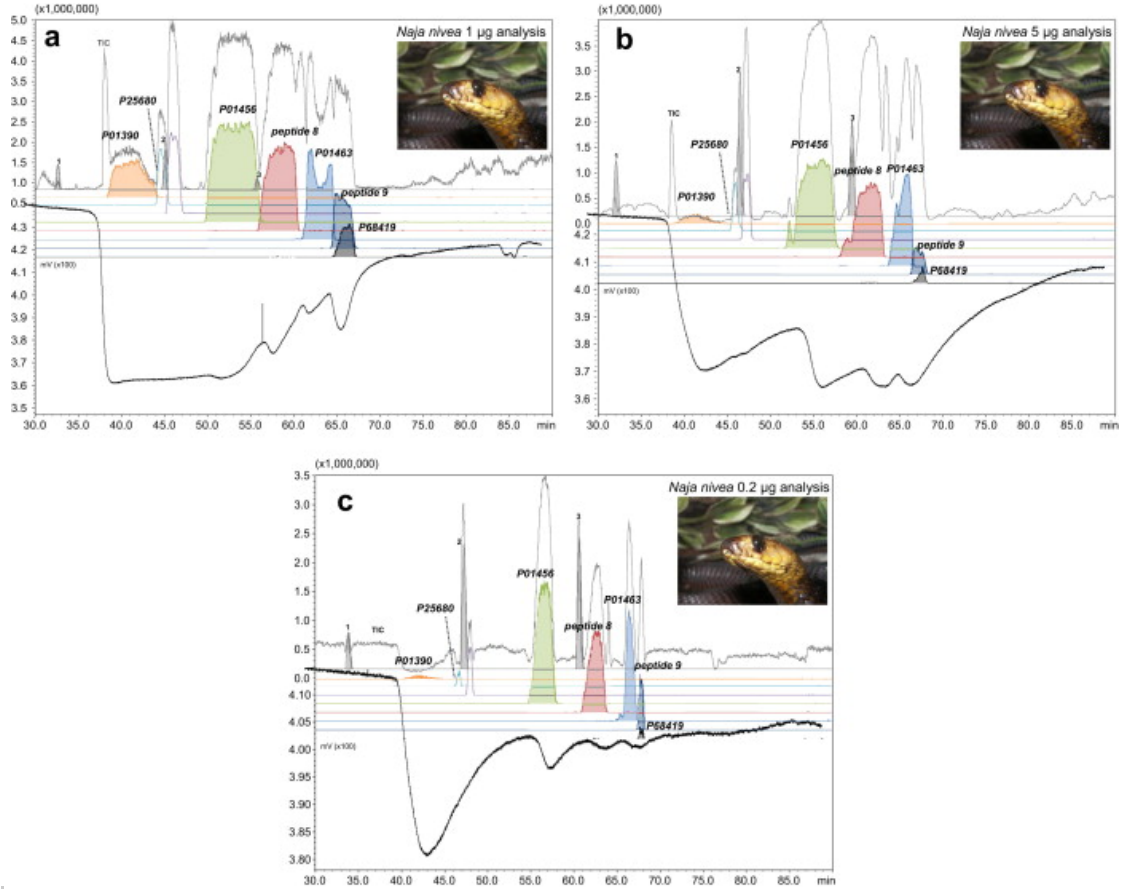

Figure 5. The subsequent injections of 5 µg, 1 µg and 0.2 µg of crude *Naja nivea* venom (A, B and C respectively) obtained at least 5 ligands. The binding signal at 39 min can be attributed to the high-affinity α-cobratoxin P01390. As this strong binder elutes from the analytical column in a very broad peak (and thereby overloading the bioaffinity signal) the remaining toxins are hard to distinguish (such as toxin P25680). From the lower concentration venom analysis it was possible to correlate at least four other toxins, of which three are classified as Type IA cytotoxins (P01456, P01463 and P68419) while the other two toxins are not reported on.

3.2.6. Snake 4: Naja nivea

N. nivea (Cape cobra) is closely related to other African cobras such as the *Naja haja* and *N. annulifera*, as can be traced back to its venom, having a high affinity α-cobratoxin and several low-affinity Ls-AChBP binders (Fig. 5A). At least five ligands could be detected from analysing 5, 1 and 0.2 µg crude venom samples, respectively. The high-affinity binder at 39 min, P01390, is a Type II α-NTX. As due to column overloading a small percentage of the total bioactive P01390 slowly elutes from the column in a tailing fashion, the Ls-AChBP affinity of the remaining neurotoxins is somewhat harder to distinguish. This again shows the potential problem of seemingly severe peak broadening when very high abundant and/or high affinity ligands are present in a venom. It has to be noted that the bioaffinity signals are sigmoidal in their response and not linear. This results in seemingly very severe peak broadening in the bioaffinity trace, while this is not observed in the parallel MS (or UV) response. This indicates that it is in fact not severe peak broadening but caused due to an intrinsic characteristic of biochemical detection in general. Closely eluting to the high-affinity binder P01390 is P25680, an orphan group II toxin. It could be a low-affinity binder, but due to the high binding signal of P01390 no conclusions can be drawn. The bioactivity signal at 53 min can be attributed to P01456, classified as a Type IA cytotoxin. The binding profile at 57 min is caused by a peptide (*peptide 8*) which could not be mass correlated with literature

data. The binding profile at 63 min is due to P01463, classified as a Type IA cytotoxin. At 67 min, the peptide that is most probably binding to AChBP is P68419, which is classified as an α1 nAChR ligand. But AChBP bioaffinity of the co-eluting *peptide 9* cannot be ruled out either. As also shown for the *D. jamesoni* and *N. annulifera* venom analyses, analysing lower concentrations of the *N. nivea* venom assists in more accurate mass correlations of bioactives, thus facilitating their identification. The data in these analyses are complementary: while the major bioactive peptides are readily detected by MS upon a 5 μg injection, their detection becomes more difficult or even impossible at 1 μg (Fig. 5B) and 0.2 μg analysis (Fig. 5C). However, in the biochemical detection, the smaller sample injections result in increased chromatographic resolution and allow the minor bioactives to be analysed more clearly.

3.2.7. Overall evaluation of results and perspectives

As discussed earlier, the AChBP is an established structural homologue of the α7 nAChR, a (potential) drug target for pain syndromes, cognitive and neurodegenerative diseases. As Type II α-NTXs are high-affinity binders to the α7 nAChR, AChBP is a valid and very useful water-soluble target model to screen for high-affinity binders in these venoms. Snake venoms might contain potential biopharmaceuticals. In case of neurotoxin venoms, particular interest is in targeting nAChRs, e.g., the α7 nAChR. Besides discovery of such potential biopharmaceuticals, screening of venoms may also yield valuable tool compounds with high affinity towards specific ion channels, which can be used as tools for biological and pharmacological studies [30, 31]. Typical examples of such snake toxin peptides are the α-bungarotoxins and α-cobratoxins [7, 13, 36]. This study showed that screening of snake venoms using the miniaturized HRS approach with the Ls-AChBP yields not only many high-affinity peptide/protein ligands, but also low-affinity Ls-AChBP ligands, which were reported as Type I α-NTXs, cardiotoxins and PLA_2s. In addition, several other bioactive peptide ligands were found that were previously unreported or reported as orphan ligands, of which the biological function is presumed only based on sequence homology.

The data obtained from screening *D. jamesoni kaimosae* venom clearly shows that ligands still can be identified even though the peptides are closely eluting in relatively broad peaks. Here, low-affinity binders are first identified by injecting a higher concentration sample, followed by an analysis of more diluted sample(s) to distinguish ligands with high affinity from low-affinity ligands. In the second Elapidae snake venom profiled, a strategy is shown in which co-eluting peptides from *N. haje annulifera* venom (of which one has a very high affinity towards Ls-AChBP) are correlated with the biochemical detection signal with higher confidence by means of changing the selectivity of the reversed-phase LC separation (by pH change in our case) followed by reanalysis of the sample. This strategy, where an additional chromatographic run was performed at a high pH, narrowed possible ligands significantly. The last example showed how a serial dilution analysis of *Naja nivea* venom enabled the detection of 5 possible AChR ligands.

As described in the method evaluation, the structure of venom peptides is highly conserved in their evolutionary trail causing their chromatographic behaviour also to be similar. Besides poor separation because of iso-toxins, also poor chromatographic peak shapes pose an analytical challenge. Even though these characteristics result in often challenging

chromatographic separations, peptide ligands could be identified by direct correlation of the biochemical detection signal with the EICs from MS as obtained from our IT–TOF MS measurements. Once correlated, these masses give an idea of the identity of peptides, e.g., Type 1 or Type 2. As the correlated masses found are accurate (measurements are performed by an accurate and high-resolution MS), these masses furthermore provide for a straightforward and targeted fractionation approach. After chromatographic purification, a validation can be performed by re-analysing the purified sample, followed by further structural elucidation by, e.g., tryptic digestion, proteomics analysis and *de novo* sequencing, Edman degradation as well as receptor binding and activation studies.

Conclusion

Animal venoms provide for numerous ligands towards a myriad of receptors, enzymes and ion channels and therefore have the intrinsic potential to modulate biological and pharmaceutically relevant signal cascades. This study describes the application of a miniaturized on-line analytical methodology where neurotoxic snake venoms (from Elapidae) are screened for toxins with Ls-AChBP affinity, mimicking binding to neuronal nAChRs, especially α7 nAChR. Prior to snake profiling, a post-column nano-split was developed and implemented followed by evaluation and validation of the methodology. The methodology proved to be suitable for the profiling of snake venoms. By correlating bioactive peptides with their mass identified, we were able to pinpoint bioactives. In many cases, toxins described in literature are only correlated to a possible function by amino-acid homology only.

We found 6 peptides that were not previously correlated with neuronal nAChR affinity and therefore are interesting molecules for further studies on their biological interactions with nAChRs. Although subsequent in depth studies of the toxins described in this study for nAChR binding are needed, their affinities towards the Ls-AChBP give a hint of their (or one of their) function(s), i.e., targeting nAChRs. Besides these orphan toxins described, also 9 unknown peptides were found, which are in need of additional sequencing and functional assaying. Even though only the long neurotoxins (Type II) have been correlated with the neuronal α7 nAChR, most of the peptides that were found in this study were short neurotoxins (60–64) amino acids. All short neurotoxins described in literature are 6700–6900 Da. Venom analysis from *D. jamesoni kaimosae* yielded two ligands known as α1 nAChR ligands, while two other binders are classified as orphan ligands. Further studies are required to validate these results, as for the six other (possible) neuronal nAChR ligands found in this venom proteome, which, to this date, are not described in literature. The main binder in the *N. annulifera* venom proteome was attributed to a known α7 nAChR binder, of a closely related Egyptian cobra, while two other distinct ligands are correlated to toxins described in literature as cardiotoxin only. The analysis of this particular venom shows the benefit of analysing at both a high and low pH, as this caused selectivity changes in the reversed-phase LC separation leading to more straightforward correlation of the bioactivity and the mass

spectrometric detection of a low-abundant, high-affinity ligand. The *Naja Nivea* venom proteome showed four distinct binding peaks which can be attributed to five ligands; the largest signal is caused by the a known α7 nAChR ligand, while the three other binding peaks can be attributed to tree ligands previously described as cardiotoxin and two unknown peptides, of which one co-elutes with one of the cardiotoxins.

The rapid and high-resolution screening of the four venom proteomes shows the potential of the here described microfluidic on-line screening methodology. Not only did the application showed the analysis speed, it also demonstrated the advantage of the direct post-column analysis. Furthermore, by the coupling of a miniaturized separation technique (nano-LC) to a microfluidic on-line assay and sensitive fluorescence detection, we showed that multiple, sensitive and robust analyses are possible in a short time frame with a minimal amount of venom used. Other soluble pharmacological targets can be implemented in the miniaturized screening platform and applied to the screening of animal venoms. As we developed many on-line screening platforms in the past [26] using various molecular targets, we are convinced that in most cases transfer to the miniaturized screening platform should be feasible. A miniaturized platform based on acetylcholine esterase with MS as bioassay readout has already been demonstrated [1]. Membrane receptors and ion channels are out of reach for on-line screening since the incompatibility of membranes in on-line systems (membranes stick to the flow through pathway), instability of the receptors to eluents used in gradient reversed phase LC, and the concentration of receptors in the membranes (usually too low). Ways to overcome this problem by nanofractionation approaches are currently under investigation [28, 32].

Acknowledgements

This work was financially supported with an ECHO grant of the Dutch Scientific Society NWO (OND1331288 ECHO number 700.56.043). ABS was partially funded by a grant from the European Union Seventh Framework Programme under grant agreement no HEALTH F2 2007 202088 (Structure, function and disease of Cys loop receptors, “NeuroCypres” project). We would like to thank Dr. Neil Loftus from Shimadzu for the collaboration and use of the Shimadzu nano-ESI source.

References

1. de Boer, A.R., B. Bruyneel, J.G. Krabbe, H. Lingeman, W. M.A. Niessen and H. Irth, (2005) A microfluidic-based enzymatic assay for bioactivity screening combined with capillary liquid chromatography and mass spectrometry. Lab Chip. **5**: 1286-92.
2. Brack, W., 2003. Effect-directed analysis: a promising tool for the identification of organic toxicants in complex mixtures? Anal. Bioanal. Chem. **377**: 397–407.
3. Brack,W., Klamer, H.J., Lopez de Alda, M., Barcelo, D., 2007. Effect-directed analysis of key toxicants in European river basins a review. Environ. Sci. Pollut. Res. Int. **14**: 30–38.
4. Celie, P.H., Kasheverov, I.E., Mordvintsev, D.Y., Hogg, R.C., van Nierop, P., van Elk, R., van Rossum-Fikkert, S.E., Zhmak, M.N., Bertrand, D., Tsetlin, V., Sixma, T.K., Smit, A.B., (2005). Crystal structure of

nicotinic acetylcholine receptor homolog AChBP in complex with an alphaconotoxin PnIA variant. Nat. Struct. Mol. Biol. **12**, 582–588.
5. Chang, L., Lin, S., Huang, H., Hsiao, M., 1999. Genetic organization of alpha-bungarotoxins from Bungarus multicinctus (Taiwan banded krait): evidence showing that the production of alpha-bungarotoxin isotoxins is not derived from edited mRNAs. Nucleic Acids Res. 27, 3970–3975.
6. Dubovskii, P.V., Lesovoy, D.M., Dubinnyi, M.A., Utkin, Y.N., Arseniev, A.S., 2003. Interaction of the P-type cardiotoxin with phospholipid membranes. Eur. J. Biochem. FEBS 270, 2038–2046.
7. Dutertre, S., Lewis, R.J., 2006. Toxin insights into nicotinic acetylcholine receptors. Biochem. Pharmacol. 72, 661–670.
8. Ebada, S.S., Edrada, R.A., Lin, W., Proksch, P., 2008. Methods for isolation, purification and structural elucidation of bioactive secondary metabolites from marine invertebrates. Nat. Protoc. 3, 1820–1831.
9. Fernandez, J., Alape-Giron, A., Angulo, Y., Sanz, L., Gutierrez, J.M., Calvete, J.J., Lomonte, B., 2011. Venomic and antivenomic analyses of the Central American coral snake, Micrurus nigrocinctus (Elapidae). J. Proteome Res. 10, 1816–1827.
10. Fiordalisi, J.J., Grant, G.A., 1993. Evidence for a fast-exchange conformational process in alpha-bungarotoxin. Toxicon 31, 767–775.
11. Fry, B.G., Wuster, W., Kini, R.M., Brusic, V., Khan, A., Venkataraman, D., Rooney, A.P., 2003. Molecular evolution and phylogeny of elapid snake venom three-finger toxins. J. Mol. Evol. 57, 110–129.
12. Gorbacheva, E.V., Starkov, V.G., Tsetlin, V.I., Utkin, Y.N., Vulfius, C.A., 2008. Viperidae snake venoms block nicotinic acetylcholine receptors and voltage-gated Ca2þ channels in identified neurons of fresh-water snail Lymnaea stagnalis. Biochem. (Mosc.) Suppl. Ser. A: Membr. Cell Biol. 2, 122–127.
13. Hansen, S.B., Radic, Z., Talley, T.T., Molles, B.E., Deerinck, T., Tsigelny, I., Taylor, P., 2002. Tryptophan fluorescence reveals conformational changes in the acetylcholine binding protein. J. Biol. Chem. 277, 41299–41302.
14. Harvey, A.L., 1985. Cardiotoxins from cobra venoms: possible mechanisms of action. Toxin Rev. 4, 41–69.
15. Harvey, A.L., 2008. Natural products in drug discovery. Drug Discov. Today 13, 894–901.
16. Heus, F., Giera, M., de Kloe, G.E., van Iperen, D., Buijs, J., Nahar, T.T., Smit, A.B., Lingeman, H., de Esch, I.J., Niessen, W.M., Irth, H., Kool, J., 2010. Development of a microfluidic confocal fluorescence detection system for the hyphenation of nano-LC to on-line biochemical assays. Anal. Bioanal. Chem. 398, 3023–3032.
17. Houtman, C.J., Booij, P., van der Valk, K.M., van Bodegom, P.M., van den Ende, F., Gerritsen, A.A., Lamoree, M.H., Legler, J., Brouwer, A., 2007. Biomonitoring of estrogenic exposure and identification of responsible compounds in bream from Dutch surface waters. Environ. Toxicol. Chem. 26, 898–907.
18. Jeyaseelan, K., Poh, S.L., Nair, R., Armugam, A., 2003. Structurally conserved alpha-neurotoxin genes encode functionally diverse proteins in the venom of Naja sputatrix. FEBS Lett. 553, 333–341.
19. Joubert, F., Taljaard, N., 1978. Purification, some properties and the primary structures of three reduced and S-carboxymethylated toxins (CM-5, CM-6 and CM-10a) from Naje haje haje (Egyptian cobra) venom. Biochim. biophys. Acta 537, 1–8.
20. Joubert, F.J., 1975. The purification and amino acid sequence of toxin CM- 13b from Naja haje annulifera (Egyptian cobra) venom. Hoppe-Seyler's Z. physiol. Chem. 356, 1901–1908.
21. Joubert, F.J., 1976. Snake venom toxins. The amino-acid sequences of three toxins (CM-8, CM-11 and CM-13a) from Naja haje annulifera (Egyptian cobra) venom. Eur. J. Biochem. FEBS 64, 219–232.
22. Kapoor, V.K., 2010. Natural toxins and their therapeutic potential. Indian J. Exp. Biol. 48, 228–237.
23. Kini, R.M., Doley, R., 2010. Structure, function and evolution of threefinger toxins: mini proteins with multiple targets. Toxicon 56, 855–867.
24. Koehn, F.E., Carter, G.T., 2005. The evolving role of natural products in drug discovery. Nat. Rev. Drug Discov. 4, 206–220.
25. Konshina, A.G., Boldyrev, I.A., Utkin, Y.N., Omel'kov, A.V., Efremov, R.G., 2011. Snake cytotoxins bind to membranes via interactions with phosphatidylserine head groups of lipids. PLoS One 6, e19064.
26. Kool, J., Giera, M., Irth, H., Niessen, W.M.A., 2011. Advances in mass spectrometry-based post-column bioaffinity profiling of mixtures. Anal. Bioanal. Chem. 399, 2655–2668.
27. Kool, J., de Kloe, G.E., Bruyneel, B., de Vlieger, J.S., Retra, K., Wijtmans, M., van Elk, R., Smit, A.B., Leurs, R., Lingeman, H., de Esch, I.J., Irth, H., 2010. Online fluorescence enhancement assay for the acetylcholine binding protein with parallel mass spectrometric identification. J. Med. Chem. 53, 4720–4730.
28. Kool, J., Rudebeck, A.F., Fleurbaaij, F., Nijmeijer, S., Falck, D., Smits, R.A., Vischer, H.F., Leurs, R., Niessen, W.M.A., 2012. High-resolution metabolic profiling towards G protein-coupled receptors: rapid and comprehensive screening of histamine H(4) receptor ligands. J. Chromatogr. A. 1259, 213–220.
29. Kumar, T.K., Jayaraman, G., Lee, C.S., Arunkumar, A.I., Sivaraman, T., Samuel, D., Yu, C., 1997. Snake venom cardiotoxins-structure, dynamics, function and folding. J. Biomol. Struct. Dyn. 15, 431–463.

30. Lewis, R.J., Garcia, M.L., 2003. Therapeutic potential of venom peptides. Nat. Rev. Drug Discov. 2, 790–802.
31. Mouhat, S., Andreotti, N., Jouirou, B., Sabatier, J.M., 2008. Animal toxins acting on voltage-gated potassium channels. Curr. Pharm. Des. 14, 2503–2518.
32. Nijmeijer, S., Vischer, H.F., Rudebeck, A.F., Fleurbaaij, F., Falck, D., Leurs, R., Niessen, W.M.A., Kool, J. 2012. Development of a profiling strategy for metabolic mixtures by combining chromatography and mass spectrometry with cell-based GPCR signaling. J. Biomol. Screen., 17: 1329-1338.
33. Nirthanan, S., Gwee, M.C., 2004. Three-finger alpha-neurotoxins and the nicotinic acetylcholine receptor, forty years on. J. Pharm. Sci. 94, 1–17.
34. Nyila, M.A., Leonard, C.M., Hussein, A.A., Lall, N., 2009. Bioactivities of Plectranthus ecklonii constituents. Nat. Prod. Commun. 4, 1177–1180.
35. Pook, C.E., McEwing, R., 2005. Mitochondrial DNA sequences from dried snake venom: a DNA barcoding approach to the identification of venom samples. Toxicon 46, 711–715.
36. Smit, A.B., Syed, N.I., Schaap, D., van Minnen, J., Klumperman, J., Kits, K.S., Lodder, H., van der Schors, R.C., van Elk, R., Sorgedrager, B., Brejc, K., Sixma, T.K., Geraerts, W.P., 2001. A glia-derived acetylcholine-binding protein that modulates synaptic transmission. Nature 411, 261–268.
37. Strydom, A.J., 1973. Snake venom toxins. The amino acid sequences of two toxins from Dendroaspis jamesoni kaimosae (Jameson's mamba) venom. Biochim. biophys. Acta 328, 491–509.
38. Vonk, F.J., Jackson, K., Doley, R., Madaras, F., Mirtschin, P.J., Vidal, N., 2011. Snake venom: from fieldwork to the clinic: recent insights into snake biology, together with new technology allowing high-throughput screening of venom, bring new hope for drug discovery. Bioessays 33, 269–279.
39. Vulfius, C.A., Gorbacheva, E.V., Starkov, V.G., Osipov, A.V., Kasheverov, I.E., Andreeva, T.V., Astashev, M.E., Tsetlin, V.I., Utkin, Y.N., 2011. An unusual phospholipase A from puff adder Bitis arietans venom– a novel blocker of nicotinic acetylcholine receptors. Toxicon 57, 787– 793.
40. Yu, S., Park, J.S., Paredes, V., Song, M.C., Baek, N.I., Lee, S.I., Lim, J.S., Cho, N.Y., Yoon, J., Baek, K., 2009. Screening and isolation of a natural dopamine D(1) receptor antagonist using cell-based assays. J. Biotechnol. 145 (3), 304–309.

Supplementary material

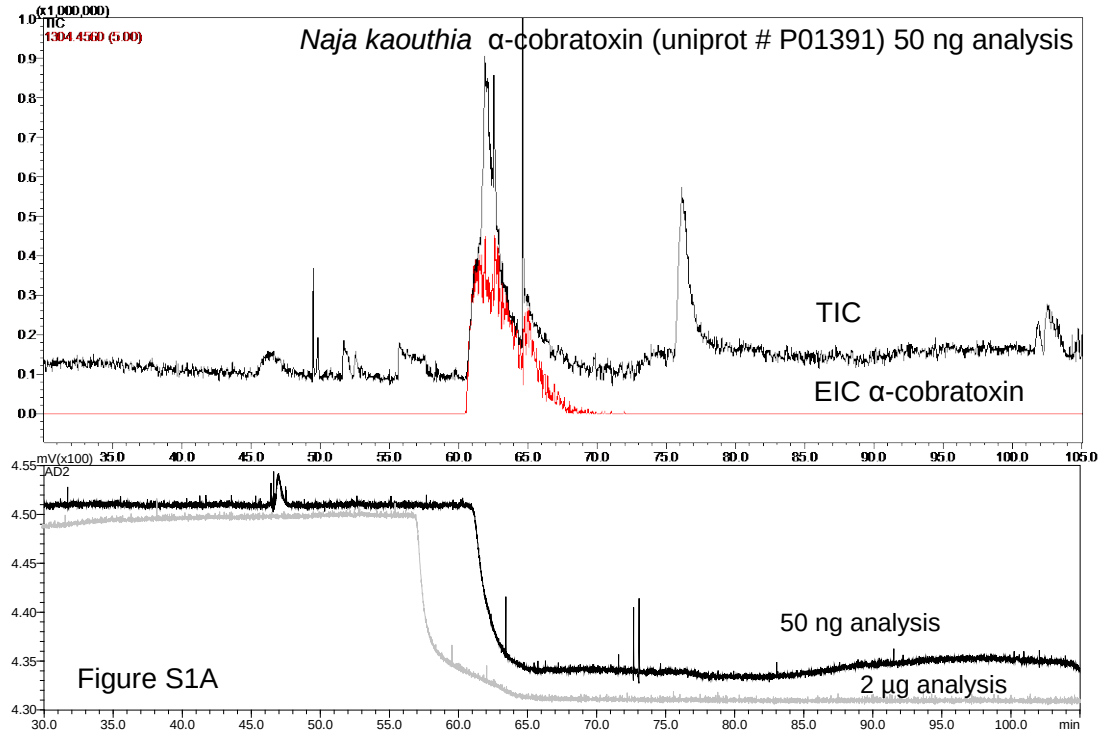

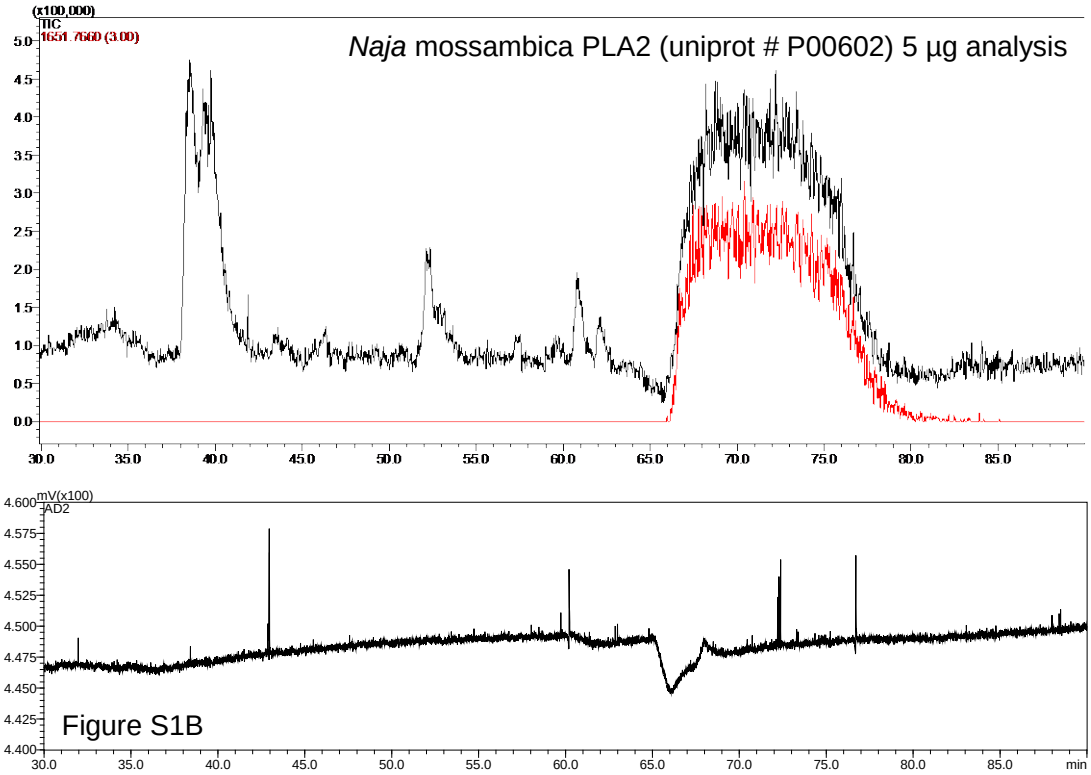

Figure S1A/B. The selectivity of the analytical setup was evaluated by injecting several short chains toxins and a phospholipase-2 toxin. The bioaffinity signals of 50 ng, and 2 µg of α-cobratoxin from *Naja kaouthia* are shown. The corresponding MS data of the 50 ng injection is also shown (S1A). The bioaffinity and MS signals of 5 µg PLA2 from *Naja mossambica* are shown (S1B).

Conus imperialis IMI conotoxin (uniprot # P50983) 500 ng analysis

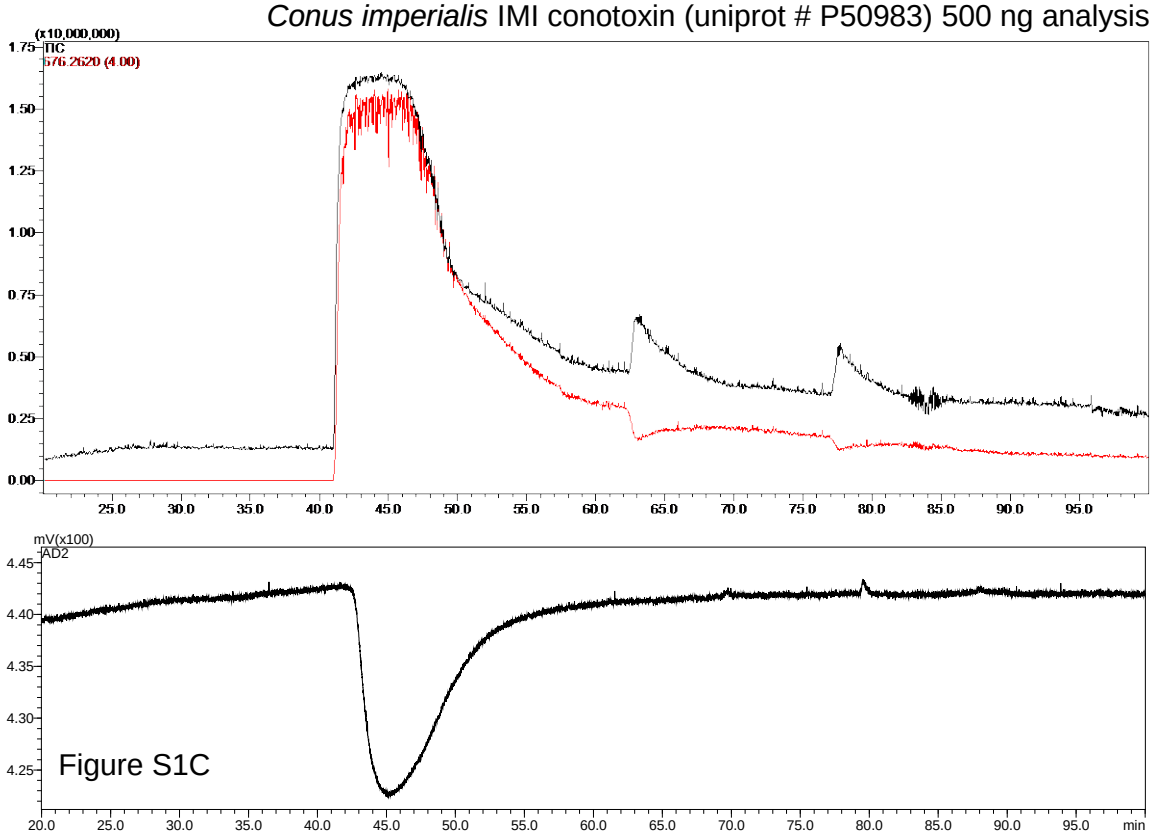

Figure S1C. The bioaffinity and MS signals of 50 ng IMI conotoxin from *Conus imperialis* are shown.